Realization of a quantum algorithm using a trapped electron

G. Ciaramicoli
Dipartimento di Fisica and INFM, Università di Roma ''La Sapienza,'' 00185 Roma, Italy

I. Marzoli and P. Tombesi
Dipartimento di Matematica e Fisica and INFM, Università di Camerino, 62032 Camerino, Italy

(Received 23 October 2000; published 16 April 2001)

We show how a single trapped electron offers the opportunity to realize universal quantum logic gates within the present experimental possibilities. As an example, we propose to implement the Deutsch algorithm by using the quantized cyclotron motion and the electron spin as qubits.

DOI: 10.1103/PhysRevA.63.052307 PACS number(s): 03.67.Lx, 03.65.−w

I. INTRODUCTION

Many theoretical proposals have presented schemes to implement quantum computation in several different physical systems: trapped ions [1], neutral atoms [2], cavity QED [3], and solid-state devices [4]. However, up to now the experimental realizations have been very few and limited to a low number of qubits. For example, in the case of trapped ions, the controlled-NOT (CNOT) quantum logic gate with two qubits has been realized [5], and more recently, entanglement of four particles has been achieved [6]. The same NMR experiments [7] are still controversial [8]. Therefore, it is worthwhile to explore other directions, searching for alternative systems, suitable for quantum logic implementation. They should fulfill two main requirements: long decoherence times and exceedingly high control from outside to manipulate the qubits and make the final readout.

Recently, an electron in a Penning trap [9] has drawn attention as a potential candidate for quantum logic operations [10]. This claim is based on the almost complete absence of decoherence mechanisms and on the experimental accuracy achieved so far. Just to mention a few facts, this system has been designed to perform the most precise measurement of the electron g factor [11] and other fundamental constants. Radiative damping is negligible, also because of cavity effects that prevent emission of synchrotron radiation [12,13]. Moreover, transitions induced by blackbody radiation become extremely unlikely below 1 K [12]. All this, very recently, has led to the nondestructive observation of Fock states for the cyclotron motion [12].

This last experimental realization motivates the present proposal. Contrary to Ref. [10], we encode the two qubits in the cyclotron and spin degrees of freedom of the electron. This choice is determined by the fact that these are the only motions that are truly quantum. Indeed, the axial oscillation and the magnetron motion are still in a classical regime, although, considering the experimental improvements, there exist possibilities that in the near future the axial motion could be cooled down to its ground state [14].

Moreover, in the present paper, the electron state preparation and manipulation rely on a completely different mechanism. Here the essential ingredient is the anharmonicity of the cyclotron motion and the coupling with the spin, due to small relativistic corrections. Once we can resolve different cyclotron and spin transitions, even conditional logic gates, like the CNOT, become feasible. Furthermore, we show how to realize one-qubit rotations, i.e., the Hadamard transform. With these elements in hand, one can already build up a small network. Indeed, two qubits are enough to implement the Deutsch algorithm and to test the performances of this prototype of quantum processor.

The paper is organized as follows. In Sec. II, we describe the physical system, with special emphasis on the relativistic corrections that affect the energy-level structure of the trapped electron. How to manipulate the electron state in a controlled way is the subject of Sec. III. We then recall, in Sec. IV, the Deutsch algorithm and the network required to implement it. Its physical realization is explained in Sec. V, where we provide a detailed explanation of how to build up universal logic gates using the cyclotron and the spin degrees of freedom. The efficiency of the measurement scheme to read out the outcomes of the computation is analyzed in Sec. VI. Finally, we summarize in Sec. VII our main results and discuss future perspectives for this system.

II. ELECTRON IN A PENNING TRAP

In this section, we briefly review the essential features of the dynamics of a single electron trapped in a Penning trap [9], the so-called *geonium atom* [13,15], in view of possible applications to quantum information processing.

The trapping mechanism relies on the combination of the electrostatic quadrupole potential

$$V(x,y,z)=V_0\frac{z^2-(x^2+y^2)/2}{2d^2}, \tag{1}$$

with the uniform magnetic field $\mathbf{B}=B\hat{\mathbf{k}}$ along the z axis. In Eq. (1), V_0 is the potential applied between the trap electrodes, while the characteristic length d is determined by the trap size

$$d^2\equiv\frac{1}{2}\left(z_0^2+\frac{r_0^2}{2}\right), \tag{2}$$

with $2z_0$ being the height of the trap and r_0 its radius.

The dynamics of a trapped electron, of charge e and mass m, is governed by the Hamiltonian

$$H_0=\frac{1}{2m}\left(\mathbf{p}-\frac{e}{c}\mathbf{A}_0\right)^2+eV-\boldsymbol{\mu}\cdot\mathbf{B}, \tag{3}$$

where $\mathbf{A}_0$ is the vector potential

$$\mathbf{A}_0(x,y)=\tfrac{1}{2}\mathbf{B}\times\mathbf{r} \tag{4}$$

and $\boldsymbol{\mu}\equiv ge\hbar/(4mc)\boldsymbol{\sigma}$ is the electron intrinsic magnetic moment, with g being the electron g factor and $\boldsymbol{\sigma}\equiv(\sigma_x,\sigma_y,\sigma_z)$ the spin operator having Pauli matrices as components.

It is convenient to introduce the following ladder operators:

$$a_z=\sqrt{\frac{m\omega_z}{2\hbar}}z+i\sqrt{\frac{1}{2\hbar m\omega_z}}p_z, \tag{5}$$

$$a_c=\frac{1}{2}\left[\sqrt{\frac{m\tilde{\omega}_c}{2\hbar}}(x-iy)+\sqrt{\frac{2}{\hbar m\tilde{\omega}_c}}(p_y+ip_x)\right], \tag{6}$$

$$a_m=\frac{1}{2}\left[\sqrt{\frac{m\tilde{\omega}_c}{2\hbar}}(x+iy)-\sqrt{\frac{2}{\hbar m\tilde{\omega}_c}}(p_y-ip_x)\right], \tag{7}$$

obeying the commutation relation $[a_i,a_j^\dagger]=\delta_{i,j}$, with $i,j=z,c,m$. These operators refer, respectively, to three harmonic oscillators, describing the quantized motion of the trapped electron. Here we have defined the frequency $\tilde{\omega}_c\equiv\sqrt{\omega_c^2-2\omega_z^2}$, connected to the cyclotron

$$\omega_c\equiv\frac{|e|B}{mc} \tag{8}$$

and to the axial oscillation frequencies

$$\omega_z\equiv\sqrt{\frac{eV_0}{md^2}}. \tag{9}$$

The new operators, Eqs. (5)–(7), allow us to recast the Hamiltonian, Eq. (3), in the more transparent form [13]

$$H_0=-\hbar\omega_m\left(a_m^\dagger a_m+\frac{1}{2}\right)+\hbar\omega_c'\left(a_c^\dagger a_c+\frac{1}{2}\right)+\hbar\omega_z\left(a_z^\dagger a_z+\frac{1}{2}\right)+\frac{\hbar}{2}\omega_s\sigma_z. \tag{10}$$

The magnetron motion takes place at frequency $\omega_m\equiv(\omega_c-\tilde{\omega}_c)/2$ around a potential hill and is, therefore, unstable as one can see from the minus sign in Eq. (10). However, this instability is fully under control, because the magnetron motion is weakly coupled to the environment. Hence, the electron does not roll down the potential hill, but remains well confined inside the trap for several months.

The frequency of the cyclotron oscillator $\omega_c'\equiv(\omega_c+\tilde{\omega}_c)/2$ is slightly different from the bare cyclotron frequency defined in Eq. (8), because of the presence of the electrostatic trapping field.

The axial motion consists of a harmonic oscillation, near the trap center, at frequency ω_z [see Eq. (9)], depending on the quadrupole potential, which provides the axial confinement.

Note that these three motions build up a well-defined hierarchy in the frequency range $\omega_m\ll\omega_z\ll\omega_c'$. Typical values [13] of the eigenfrequencies are $\omega_m/(2\pi)\simeq 12$ kHz, $\omega_z/(2\pi)\simeq 64$ MHz, and $\omega_c'/(2\pi)\simeq 164$ GHz.

Beside these external degrees of freedom, there is an internal degree of freedom, the spin, which precedes around the magnetic field at the frequency

$$\omega_s\equiv\frac{g}{2}\frac{|e|B}{mc}. \tag{11}$$

Here we recall that, due to the electron anomaly, the factor g is different from the value 2 and the spin precession frequency ω_s is experimentally distinguishable [13] from the cyclotron frequency ω_c, presented in Eq. (8).

From the Hamiltonian Eq. (10), it is easy to realize that the energy levels of an electron in a Penning trap are given by

$$E_0(n,k,l,s)=-\hbar\omega_m\left(l+\frac{1}{2}\right)+\hbar\omega_c'\left(n+\frac{1}{2}\right)+\hbar\omega_z\left(k+\frac{1}{2}\right)+\frac{\hbar\omega_s}{2}s, \tag{12}$$

where the four quantum numbers $l=0,1,2,\ldots$, $n=0,1,2,\ldots$, $k=0,1,2,\ldots$, and $s=\pm 1$ define, respectively, the magnetron, cyclotron, axial, and spin states.

In typical experimental configurations [13], the axial harmonic oscillator is coupled to an external detection circuit, which heats up this motion. However, switching off the interaction with the measurement device, one could cool the axial motion down to 80 mK [12]. This implies that at the thermal equilibrium, the average axial quantum number k is of the order of 30. So this motion is still in the classical regime. The same conclusion applies to the magnetron motion, whose temperature is controlled by means of a sideband cooling technique [13]. The situation is, instead, quite different for the cyclotron motion, which has been recently prepared in the lowest Fock states $|n\rangle_c$, with n ranging from 0 to 4 [12]. Extremely remarkable is the fact that below 1 K, the cyclotron motion remains in its ground state for an indefinite time and in the first excited state for 13 s [12].

In this paper, we will focus only on the true quantum motions of the electron, namely the cyclotron oscillator and the spin, with the aim of using them as registers for quantum information. The electron spin, being a two-level system, lends itself quite naturally to encode the logical states $|0\rangle$ and $|1\rangle$. Instead, it is not so obvious to implement a qubit in a multilevel system like a harmonic oscillator with equally spaced energy levels. This is, unfortunately, the case of the cyclotron motion. A possible way to circumvent this problem is to introduce some kind of anharmonicity in order to address a specific transition between two energy levels.

Actually, before perturbing this simple system from outside, we can consider the intrinsic sources of anharmonicity. Such an analysis has been already done [13] because of the exceedingly high precision spectroscopy experiments carried out on the geonium. The main corrections to the Hamiltonian Eq. (10) are produced by the relativistic effects [16,17] and by the departures of the actual electrostatic field from the ideal quadrupole potential of Eq. (1). These effects, treated in perturbation theory, result in the following corrections to the energy levels of Eq. (12):

$$\Delta E(n,k,l,s)\approx\frac{eV_0C_4\hbar^2}{2d^4m^2}\left\{\frac{3}{2\omega_z^2}\left(k^2+k+\frac{1}{2}\right)-\frac{3}{\omega_z(\omega_c'-\omega_m)}(2k+1)(n+l+1)+\frac{3}{2(\omega_c'-\omega_m)^2}\left[\left(n+\frac{1}{2}\right)^2+\left(l+\frac{1}{2}\right)^2\right.\right.$$
$$\left.\left.+4\left(n+\frac{1}{2}\right)\left(l+\frac{1}{2}\right)+\frac{1}{2}\right]\right\}-\frac{(\hbar\omega_c')^2}{2mc^2}\left[\frac{n+1/2+(\omega_m/\omega_c')^2(l+1/2)}{1-\omega_m/\omega_c'}+\frac{1}{2}\frac{\omega_z}{\omega_c'}\left(k+\frac{1}{2}\right)+\frac{1}{2}\frac{\omega_c}{\omega_c'}s\right]^2$$
$$-\frac{\hbar^2\omega_z^4}{4mc^2(\omega_c'-\omega_m)^2}\left[\left(n+\frac{1}{2}\right)\left(l+\frac{1}{2}\right)-\frac{1}{4}\right]-\frac{(\hbar\omega_z)^2}{16mc^2}\left[\left(k+\frac{1}{2}\right)^2+\frac{3}{4}\right]$$
$$+(1+2a)\frac{(\hbar\omega_z)^2}{4mc^2}s\frac{n+1/2+(\omega_m/\omega_c')(l+1/2)}{1-\omega_m/\omega_c'}-\frac{a\hbar^2\omega_c\omega_z s}{4mc^2}\left(k+\frac{1}{2}\right),\tag{13}$$

where $a\equiv(g-2)/2$ is the electron anomaly and C_4 is a constant depending on the geometrical properties of the trap and on the additional potential applied to compensation electrodes.

On the right-hand side of Eq. (13), the first term in curly brackets is the energy shift due to the electrostatic effects while the other terms are the energy shifts due to the relativistic effects. These corrections makes the three oscillators, describing the electron motion inside the trap, anharmonic, i.e., their energy levels are no longer equally spaced.

For the cyclotron oscillator, the transition frequency between neighboring levels of quantum numbers $n+1$ and n, in typical experimental configurations, becomes, neglecting the smaller terms of Eq. (13) and setting $\omega_m/\omega_c'\simeq 0$,

$$\omega_c(n,s)\equiv\frac{E(n+1,k,l,s)-E(n,k,l,s)}{\hbar}$$
$$\approx\omega_c'-\delta(n+1)-\frac{\delta}{2}s,\tag{14}$$

where $E(n,k,l,s)=E_0(n,k,l,s)+\Delta E(n,k,l,s)$ and $\delta\equiv\hbar\omega_c^2/(mc^2)$. Equation (14) shows that the cyclotron transition frequency depends on the quantum numbers n and s. Hence, the relativistic effects turn on an interaction between the cyclotron and the spin motion. Consequently, under the same assumptions, we find that the spin-flip frequency

$$\omega_s(n)\equiv\frac{E(n,k,l,+1)-E(n,k,l,-1)}{\hbar}\approx\omega_s-\delta\left(n+\frac{1}{2}\right)\tag{15}$$

depends on the cyclotron excitation n.

These considerations are better illustrated by a schematic view of the energy levels of the system presented in Fig. 1. Here and in the remainder of the paper, we neglect the dependence on the magnetron m and axial k quantum numbers, since the magnetron motion is essentially decoupled from the other electronic degrees of freedom and the axial oscillation is only relevant to the final measurement process. A discussion of this last step is postponed to Sec. VI. Therefore, in Fig. 1, we restrict the energy-level scheme to the low-lying cyclotron and spin levels. Note that different cyclotron or spin transition frequencies differ by multiples of $\delta/2\pi\approx 200$ Hz. This is a very small shift compared to the characteristic cyclotron and spin frequencies, which are of the order of 160 GHz. In principle, cyclotron and spin individual transitions are resolvable because the corresponding natural linewidths, due to radiative decay [13], are much narrower. However, a careful analysis requires us to take into account

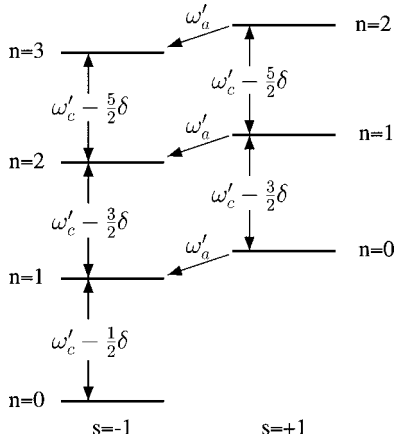

FIG. 1. Energy-level scheme (not to scale) of cyclotron, $n=0,1,2,3,\ldots$, and spin, $s=\pm 1$, motion, including the relativistic corrections discussed in Eq. (13). The transition at the anomaly frequency ω_a' produces an exchange of energy between the cyclotron motion and the spin.

even the extremely small coupling to the axial motion introduced by the relativistic corrections [see Eq. (13)]. This is a source of fluctuations, because, as mentioned before, the axial motion is in a thermal state. To minimize the consequent line-shape broadening, it is necessary to cool the axial motion as much as possible. This is done when the axial oscillator is isolated from its environment, i.e., from the external detection circuit.

In the next section, we take advantage of the anharmonicity of the cyclotron oscillator and of the dependence of the spin-flip transition frequency on the cyclotron state, to coherently manipulate the electron state inside the Penning trap.

III. PREPARATION OF THE ELECTRON STATE

The relativistic effects are mainly responsible for the energy shifts discussed at the end of the preceding section. In particular, the cyclotron energy levels are no longer equally spaced, as happens, instead, for a harmonic oscillator. This fact opens up the possibility to address transitions between specific levels. To this end, we need a tunable microwave source interacting with the trapped electron.

A very convenient trap geometry is represented by the cylindrical one [18,19], because it acts like a cylindrical microwave cavity with well-characterized radiation modes [20–22]. This latest generation of traps presents the advantage, over traditional hyperbolic traps, of better control of the electron-cavity interaction. A fundamental effect due to the cavity presence is the inhibition of synchrotron radiation when the cyclotron oscillation frequency is tuned away from any cavity mode. A cyclotron Fock state lifetime of 13 s has been observed [12], which is 140 times longer than the expected value in free space. Moreover, the electron remains in the cyclotron ground state until a resonant driving field is injected into the trap. We are, therefore, confident that a properly designed sequence of pulses can manipulate the electron state in a controlled way. More precisely, we consider an external microwave source exciting the cyclotron motion. The linearly polarized driving field is represented by means of the vector potential

$$\mathbf{A}_{\rm ext} = -\mathcal{A}\sin(\Omega t-\varphi)\hat{\imath}, \tag{16}$$

where $\mathcal{A}$ and Ω are, respectively, the amplitude and the frequency of the wave. We neglect the spatial dependence of the external field because the electron motion is confined to a region much smaller than the wavelength of the radiation in the microwave range. This fact allows us to use the dipole approximation.

Hence, the Hamiltonian of the system, Eq. (3), should be accordingly modified in order to include the applied external field

$$H \simeq H_0 - \frac{e}{mc}\mathbf{p}\cdot\mathbf{A}_{\rm ext} + \frac{e^2}{mc^2}\mathbf{A}_0\cdot\mathbf{A}_{\rm ext}, \tag{17}$$

where we neglected the term proportional to $\mathbf{A}_{\rm ext}^2$. For frequencies Ω of the external field close to the frequency ω_c' of the cyclotron oscillator, the relevant part of the system Hamiltonian, in the interaction picture, can be written as

$$H_{IP}^{(\rm cycl)} \simeq \mathcal{A}\left(\frac{|e|}{4mc}\sqrt{\frac{\hbar m\tilde{\omega}_c}{2}} + \frac{e^2B}{4mc^2}\sqrt{\frac{\hbar}{2m\tilde{\omega}_c}}\right) \times (a_c e^{-i\varphi} + a_c^\dagger e^{i\varphi}). \tag{18}$$

Thus, by carefully tuning the source frequency to the value $\omega_c(n=0,s=-1)=\omega_c'-\delta/2$ (see Fig. 1) and applying the drive for a time t, we excite only transitions between the following levels:

$$|0\rangle_c|\downarrow\rangle \rightarrow \left[\cos\left(\frac{\eta t}{2}\right)|0\rangle_c - ie^{i\varphi}\sin\left(\frac{\eta t}{2}\right)|1\rangle_c\right]|\downarrow\rangle, \tag{19}$$

$$|1\rangle_c|\downarrow\rangle \rightarrow \left[\cos\left(\frac{\eta t}{2}\right)|1\rangle_c - ie^{-i\varphi}\sin\left(\frac{\eta t}{2}\right)|0\rangle_c\right]|\downarrow\rangle, \tag{20}$$

where the Rabi frequency is

$$\eta \equiv \frac{\mathcal{A}}{\hbar}\left(\frac{|e|}{2mc}\sqrt{\frac{\hbar m\tilde{\omega}_c}{2}} + \frac{e^2B}{2mc^2}\sqrt{\frac{\hbar}{2m\tilde{\omega}_c}}\right) \tag{21}$$

and $|n\rangle_c$, $|\downarrow\rangle$ ($|\uparrow\rangle$) indicate, respectively, the cyclotron state with excitation number n and the spin-down (-up) state. We define the above interaction as a $p_{c(1/2)}(\eta t,\varphi)$ pulse.

From Fig. 1, we also see, in the same way, that when the external source frequency is on resonance with $\omega_c(n=0,s=+1)=\omega_c'-3\delta/2$, we couple two different pairs of cyclotron levels,

$$|1\rangle_c|\downarrow\rangle \rightarrow \left[\cos\left(\sqrt{2}\,\frac{\eta t}{2}\right)|1\rangle_c - ie^{i\varphi}\sin\left(\sqrt{2}\,\frac{\eta t}{2}\right)|2\rangle_c\right]|\downarrow\rangle, \tag{22}$$

$$|2\rangle_c|\downarrow\rangle \rightarrow \left[\cos\left(\sqrt{2}\,\frac{\eta t}{2}\right)|2\rangle_c - ie^{-i\varphi}\sin\left(\sqrt{2}\,\frac{\eta t}{2}\right)|1\rangle_c\right]|\downarrow\rangle, \tag{23}$$

$$|0\rangle_c|\uparrow\rangle \rightarrow \left[\cos\left(\frac{\eta t}{2}\right)|0\rangle_c - ie^{i\varphi}\sin\left(\frac{\eta t}{2}\right)|1\rangle_c\right]|\uparrow\rangle, \tag{24}$$

$$|1\rangle_c|\uparrow\rangle \rightarrow \left[\cos\left(\frac{\eta t}{2}\right)|1\rangle_c - ie^{-i\varphi}\sin\left(\frac{\eta t}{2}\right)|0\rangle_c\right]|\uparrow\rangle. \tag{25}$$

We denote the above interaction as a $p_{c(3/2)}(\eta t,\varphi)$ pulse.

We have seen how the interaction between the electron and an external microwave source provides a tool to control the cyclotron state, leaving the spin unaffected. Then we need another mechanism to manipulate the electron spin. The required interaction is obtained by applying, inside the trap, a small magnetic field **b**, which lies in the xy plane and oscillates at a frequency close to the spin resonance ω_s [13],

$$\mathbf{b}(t) = b[\hat{\imath}\cos(\omega t+\theta) + \hat{\jmath}\sin(\omega t+\theta)]. \tag{26}$$

In this case, the relevant part of the system Hamiltonian becomes, in the interaction picture (IP),

$$H_{\mathrm{IP}}^{(\mathrm{spin})} \simeq \hbar \frac{\chi}{2}(\sigma_+ e^{-i\theta} + \sigma_- e^{i\theta}), \tag{27}$$

where the Rabi frequency is $\chi \equiv g|e|b/(2mc)$ and $\sigma_\pm \equiv (\sigma_x \pm i\sigma_y)/2$. If the small magnetic field is applied for a time t and has a sufficiently narrow bandwidth centered around the value $\omega_s(n=0)=\omega_s-\delta/2$, it produces a spin flip only if the cyclotron state is $|0\rangle_c$,

$$|0\rangle_c|\downarrow\rangle \rightarrow |0\rangle_c\left[\cos\left(\frac{\chi t}{2}\right)|\downarrow\rangle - ie^{-i\theta}\sin\left(\frac{\chi t}{2}\right)|\uparrow\rangle\right], \tag{28}$$

$$|0\rangle_c|\uparrow\rangle \rightarrow |0\rangle_c\left[\cos\left(\frac{\chi t}{2}\right)|\uparrow\rangle - ie^{i\theta}\sin\left(\frac{\chi t}{2}\right)|\downarrow\rangle\right]. \tag{29}$$

We define this interaction as a $p_{s0}(\chi t,\theta)$ pulse.

When, instead, the oscillating transverse magnetic field is tuned on resonance with $\omega_s(n=1)=\omega_s-3\delta/2$, the spin flip takes place only if the cyclotron state is $|1\rangle_c$,

$$|1\rangle_c|\downarrow\rangle \rightarrow |1\rangle_c\left[\cos\left(\frac{\chi t}{2}\right)|\downarrow\rangle - ie^{-i\theta}\sin\left(\frac{\chi t}{2}\right)|\uparrow\rangle\right], \tag{30}$$

$$|1\rangle_c|\uparrow\rangle \rightarrow |1\rangle_c\left[\cos\left(\frac{\chi t}{2}\right)|\uparrow\rangle - ie^{i\theta}\sin\left(\frac{\chi t}{2}\right)|\downarrow\rangle\right]. \tag{31}$$

This interaction is defined as a $p_{s1}(\chi t,\theta)$ pulse.

It is important to note that the two pulses shown above execute transformations on the spin states controlled by the cyclotron state. This suggests the possibility of performing conditional logic operations, which involve the cyclotron and the spin states, in a very straightforward way. We recall, therefore, in the next section a basic quantum algorithm and the universal logic gates required to realize it.

IV. THE DEUTSCH ALGORITHM

The Deutsch algorithm [23,24] is the simplest quantum algorithm, nevertheless it is important because it shows us the computing power of a quantum device.

Let us consider a Boolean function f that maps $\{0,1\} \rightarrow \{0,1\}$. There are exactly four functions of this type: two constant functions

$$f_1(0)=f_1(1)=0, \tag{32}$$

$$f_2(0)=f_2(1)=1; \tag{33}$$

and two balanced functions

$$f_3(0)=0, \quad f_3(1)=1, \tag{34}$$

$$f_4(0)=1, \quad f_4(1)=0. \tag{35}$$

Is it possible, by computing f only once, to find out whether it is constant or balanced, i.e., whether the binary numbers $f(0)$ and $f(1)$ are the same or different?

Classical intuition tells us that we have to evaluate both $f(0)$ and $f(1)$, that is, to compute f twice, to give a conclusive answer to the previous question. This is not so when one resorts to quantum mechanics and to its most peculiar features, such as entanglement and superposition. Indeed, a quantum algorithm allows us to solve the problem with a single function evaluation.

According to the Deutsch algorithm, we should simply perform the following operations: (i) We take two qubits and prepare them in the product state $|0\rangle|1\rangle$; (ii) we apply to each qubit the unitary Hadamard transformation $\mathcal{H}$, which produces the superposition states

$$|0\rangle \rightarrow \frac{1}{\sqrt{2}}(|0\rangle+|1\rangle), \tag{36}$$

$$|1\rangle \rightarrow \frac{1}{\sqrt{2}}(|0\rangle-|1\rangle); \tag{37}$$

(iii) we evaluate the unknown function on the first qubit and then store the result in the second qubit in the following way:

$$|x\rangle|y\rangle \rightarrow |x\rangle|f(x)\oplus y\rangle. \tag{38}$$

(the symbol $\oplus$ indicates addition modulo 2); (iv) we apply again the transformation $\mathcal{H}$ to each qubit; and (v) we perform a measurement on the first qubit. If the first qubit is in the state $|0\rangle$, the function is constant; if it is in the state $|1\rangle$, the function is balanced.

Describing the algorithm in detail, the application of the Hadamard transform $\mathcal{H}$ to each qubit of the initial state realizes

$$|0\rangle|1\rangle \rightarrow \tfrac{1}{2}(|0\rangle+|1\rangle)(|0\rangle-|1\rangle). \tag{39}$$

Then the evaluation of the unknown function produces

$$\begin{aligned}\tfrac{1}{2}(|0\rangle+|1\rangle)(|0\rangle-|1\rangle) \rightarrow \tfrac{1}{2}\{&|0\rangle[|f(0)\rangle-|1\oplus f(0)\rangle] \\ &+|1\rangle[|f(1)\rangle \quad -|1\oplus f(1)\rangle]\}.\end{aligned} \tag{40}$$

At this stage, depending on which function we consider, we have four possible outcomes. Finally, by applying once again the Hadamard transform $\mathcal{H}$ to each qubit, we obtain

$$\tfrac{1}{2}[|0\rangle(|0\rangle-|1\rangle)+|1\rangle(|0\rangle-|1\rangle)] \rightarrow |0\rangle|1\rangle \quad \text{for } f_1, \tag{41}$$

$$\tfrac{1}{2}[|0\rangle(|1\rangle-|0\rangle)+|1\rangle(|1\rangle-|0\rangle)] \rightarrow -|0\rangle|1\rangle \quad \text{for } f_2, \tag{42}$$

$$\tfrac{1}{2}[|0\rangle(|0\rangle-|1\rangle)+|1\rangle(|1\rangle-|0\rangle)] \rightarrow |1\rangle|1\rangle \quad \text{for } f_3, \tag{43}$$

$$\tfrac{1}{2}[|0\rangle(|1\rangle-|0\rangle)+|1\rangle(|0\rangle-|1\rangle)] \rightarrow -|1\rangle|1\rangle \quad \text{for } f_4. \tag{44}$$

We emphasize that, regardless of the specific Boolean function implemented, the second qubit always ends up in state $|1\rangle$. However, even though it does not convey any information on the parity properties of the function, it may turn out to be useful to check for eventual errors taking place in a real experiment.

We then move to analyze how this mathematical procedure can be implemented using an electron in a Penning trap.

V. REALIZATION OF THE DEUTSCH ALGORITHM

In order to implement the Deutsch algorithm using a single trapped electron, we store the quantum information in the cyclotron motion and in the spin degree of freedom of the electron. We identify the first two cyclotron states $|0\rangle_c, |1\rangle_c$ with the logic states $|0\rangle, |1\rangle$ of the first qubit, while the spin states $|\downarrow\rangle, |\uparrow\rangle$ represent, respectively, the logic states $|0\rangle, |1\rangle$ of the second qubit.

In the remainder of this section, we describe in detail how to realize the logic operations, which build up this algorithm, by means of the external driving fields introduced in Sec. III.

A. Performing the Hadamard transform

The Hadamard transform [see Eqs. (36) and (37)] is a one-qubit fundamental logic gate, which should be applied separately to the cyclotron and spin states. It essentially produces a rotation of the two logic states $|0\rangle$ and $|1\rangle$.

As shown in Sec. III, an external microwave field provides a tool to manipulate the cyclotron state, without changing the spin state. However, the relativistic corrections are not able to lift completely the degeneracy between transition frequencies. From Fig. 1 and Eqs. (22)–(25), one realizes that an external microwave source at frequency $\omega_c' - 3\delta/2$ excites, unfortunately, also an unwanted transition to the cyclotron state $|2\rangle_c$. In order not to populate extra cyclotron levels, we are then compelled to play with the electron spin, too. Therefore, the transformation $\mathcal{H}$ on the cyclotron qubit, the first qubit of our network, is implemented by means of the following six pulses: (i) A $p_{c(1/2)}(\pi,\pi)$ pulse; (ii) a $p_{c(1/2)}(\pi/2,-\pi/2)$ pulse; (iii) a multifrequency pulse consisting of the two pulses $p_{s0}(\pi,\pi/2)$, $p_{s1}(\pi,\pi/2)$; (iv) a $p_{c(1/2)}(\pi,\pi)$ pulse; (v) a $p_{c(1/2)}(\pi/2,-\pi/2)$ pulse; and (vi) a multifrequency pulse consisting of the two pulses $p_{s0}(\pi, -\pi/2)$, $p_{s1}(\pi,-\pi/2)$. To show how this procedure works, we consider the most general two-qubit state of the system,

$$c_1|0\rangle_c|\downarrow\rangle + c_2|1\rangle_c|\downarrow\rangle + c_3|0\rangle_c|\uparrow\rangle + c_4|1\rangle_c|\uparrow\rangle. \quad (45)$$

The application of the first two pulses affects the cyclotron states only if the spin state is down. According to Eqs. (19) and (20), it yields

$$c_1\frac{i}{\sqrt{2}}(|0\rangle_c+|1\rangle_c)|\downarrow\rangle + c_2\frac{i}{\sqrt{2}}(|0\rangle_c-|1\rangle_c)|\downarrow\rangle + c_3|0\rangle_c|\uparrow\rangle + c_4|1\rangle_c|\uparrow\rangle. \quad (46)$$

With the third pulse we flip the spin states, as shown in Eqs. (28)–(31),

$$-c_1\frac{i}{\sqrt{2}}(|0\rangle_c+|1\rangle_c)|\uparrow\rangle - c_2\frac{i}{\sqrt{2}}(|0\rangle_c-|1\rangle_c)|\uparrow\rangle + c_3|0\rangle_c|\downarrow\rangle + c_4|1\rangle_c|\downarrow\rangle. \quad (47)$$

The fourth and fifth pulse are identical, respectively, to the first two and produce

$$-c_1\frac{i}{\sqrt{2}}(|0\rangle_c+|1\rangle_c)|\uparrow\rangle - c_2\frac{i}{\sqrt{2}}(|0\rangle_c-|1\rangle_c)|\uparrow\rangle + c_3\frac{i}{\sqrt{2}}(|0\rangle_c+|1\rangle_c)|\downarrow\rangle + c_4\frac{i}{\sqrt{2}}(|0\rangle_c-|1\rangle_c)|\downarrow\rangle. \quad (48)$$

Finally, the sixth pulse flips the spin states again, obtaining

$$c_1\frac{i}{\sqrt{2}}(|0\rangle_c+|1\rangle_c)|\downarrow\rangle + c_2\frac{i}{\sqrt{2}}(|0\rangle_c-|1\rangle_c)|\downarrow\rangle + c_3\frac{i}{\sqrt{2}}(|0\rangle_c+|1\rangle_c)|\uparrow\rangle + c_4\frac{i}{\sqrt{2}}(|0\rangle_c-|1\rangle_c)|\uparrow\rangle. \quad (49)$$

It is easy to see that we have globally performed the Hadamard transform $\mathcal{H}$ on the cyclotron qubit.

We now consider the implementation of the same transformation on the spin qubit, i.e., the second qubit. The small transverse magnetic field, discussed in Sec. III, carries out this task in a very quick way. Indeed, by applying two multifrequency pulses, namely (i) a multifrequency pulse consisting of the two pulses $p_{s0}(\pi,\pi)$ and $p_{s1}(\pi,\pi)$; and (ii) a multifrequency pulse consisting of the two pulses $p_{s0}(\pi/2,\pi/2)$ and $p_{s1}(\pi/2,\pi/2)$, we are able to prepare the spin in a superposition state, regardless to the corresponding cyclotron excitation,

$$|\downarrow\rangle \rightarrow \frac{i}{\sqrt{2}}(|\downarrow\rangle+|\uparrow\rangle), \quad (50)$$

$$|\uparrow\rangle \rightarrow \frac{i}{\sqrt{2}}(|\downarrow\rangle-|\uparrow\rangle). \quad (51)$$

This operation corresponds to the Hadamard transform $\mathcal{H}$ on the second qubit, apart from an overall phase factor.

B. Performing the Boolean function evaluation

The second step of Deutsch algorithm requires us to evaluate the Boolean function f on the first qubit and to add the result to the second one, as is shown in Eq. (38). This operation, when $f=f_1$, reduces to the identity, that is,

$$|0\rangle_c|\downarrow\rangle \rightarrow |0\rangle_c|\downarrow\rangle, \quad (52)$$

$$|0\rangle_c|\uparrow\rangle \rightarrow |0\rangle_c|\uparrow\rangle, \quad (53)$$

$$|1\rangle_c|\downarrow\rangle \rightarrow |1\rangle_c|\downarrow\rangle, \quad (54)$$

$$|1\rangle_c|\uparrow\rangle \rightarrow |1\rangle_c|\uparrow\rangle. \quad (55)$$

So to evaluate f_1, we have to do nothing.

Considering the other constant function f_2, its evaluation is equivalent to a NOT gate applied to the second qubit,

$$|0\rangle_c|\downarrow\rangle \rightarrow |0\rangle_c|\uparrow\rangle, \tag{56}$$

$$|0\rangle_c|\uparrow\rangle \rightarrow |0\rangle_c|\downarrow\rangle, \tag{57}$$

$$|1\rangle_c|\downarrow\rangle \rightarrow |1\rangle_c|\uparrow\rangle, \tag{58}$$

$$|1\rangle_c|\uparrow\rangle \rightarrow |1\rangle_c|\downarrow\rangle. \tag{59}$$

Indeed, we see that the spin is flipped regardless of the value of the corresponding cyclotron excitation. To implement the above transformation, we need to apply the small transverse magnetic field long enough to flip the spin. This is achieved by means of the following two pulses.

(i) A $p_{s0}(\pi,\pi)$ pulse flips the spin when the cyclotron is in state $|0\rangle_c$,

$$|0\rangle_c|\downarrow\rangle \rightarrow i|0\rangle_c|\uparrow\rangle, \tag{60}$$

$$|0\rangle_c|\uparrow\rangle \rightarrow i|0\rangle_c|\downarrow\rangle; \tag{61}$$

(ii) a $p_{s1}(\pi,\pi)$ pulse flips the spin when the cyclotron is in state $|1\rangle_c$,

$$|1\rangle_c|\downarrow\rangle \rightarrow i|1\rangle_c|\uparrow\rangle, \tag{62}$$

$$|1\rangle_c|\uparrow\rangle \rightarrow i|1\rangle_c|\downarrow\rangle. \tag{63}$$

An overall phase factor apart, the above pulses perform the requested NOT operation on the spin qubit.

The evaluation of the balanced function f_3 produces the transformations

$$|0\rangle_c|\downarrow\rangle \rightarrow |0\rangle_c|\downarrow\rangle, \tag{64}$$

$$|0\rangle_c|\uparrow\rangle \rightarrow |0\rangle_c|\uparrow\rangle, \tag{65}$$

$$|1\rangle_c|\downarrow\rangle \rightarrow |1\rangle_c|\uparrow\rangle, \tag{66}$$

$$|1\rangle_c|\uparrow\rangle \rightarrow |1\rangle_c|\downarrow\rangle. \tag{67}$$

We point out that the spin is flipped only if the cyclotron state is $|1\rangle_c$. This kind of conditional logic operation is a so-called controlled-NOT (CNOT), in which the first qubit acts as the controller, while the second qubit is the target. In our system, this two-qubit logic gate may be implemented with just two pulses: (i) A $p_{s1}(\pi,\pi/2)$ pulse, and (ii) a $p_{c(5/2)}(2\pi,\varphi)$ pulse with arbitrary phase and in resonance with the transition frequency $\omega_c' - 5\delta/2$. As a matter of fact, starting from the generic two-qubit state,

$$c_1|0\rangle_c|\downarrow\rangle + c_2|1\rangle_c|\downarrow\rangle + c_3|0\rangle_c|\uparrow\rangle + c_4|1\rangle_c|\uparrow\rangle, \tag{68}$$

the first pulse, flipping the spin state only if the cyclotron oscillator is in the state $|1\rangle_c$, transforms the initial state into

$$c_1|0\rangle_c|\downarrow\rangle - c_2|1\rangle_c|\uparrow\rangle + c_3|0\rangle_c|\uparrow\rangle + c_4|1\rangle_c|\downarrow\rangle. \tag{69}$$

We then need the second pulse to correct the minus sign in front of the coefficient c_2. Indeed, this pulse acts only on the state $|1\rangle_c|\uparrow\rangle$, changing its phase factor during a complete Rabi cycle,

$$c_1|0\rangle_c|\downarrow\rangle + c_2|1\rangle_c|\uparrow\rangle + c_3|0\rangle_c|\uparrow\rangle + c_4|1\rangle_c|\downarrow\rangle. \tag{70}$$

Finally, we consider the evaluation of the other balanced function f_4, which gives rise to the following transformations:

$$|0\rangle_c|\downarrow\rangle \rightarrow |0\rangle_c|\uparrow\rangle, \tag{71}$$

$$|0\rangle_c|\uparrow\rangle \rightarrow |0\rangle_c|\downarrow\rangle, \tag{72}$$

$$|1\rangle_c|\downarrow\rangle \rightarrow |1\rangle_c|\downarrow\rangle, \tag{73}$$

$$|1\rangle_c|\uparrow\rangle \rightarrow |1\rangle_c|\uparrow\rangle. \tag{74}$$

These operations are equivalent to a CNOT in which the target qubit, i.e., the spin, changes state when the controller, i.e., the cyclotron, is in state $|0\rangle_c$ rather than $|1\rangle_c$. However, its implementation is not so straightforward as in the case of function f_3. In the present case, we need five pulses: (i) A $p_{s0}(\pi,-\pi/2)$ pulse to flip the spin when the cyclotron is in state $|0\rangle_c$; (ii) a $p_{c(1/2)}(2\pi,\varphi)$ pulse with arbitrary phase to change the phase factor of cyclotron states with spin down during a complete Rabi cycle; (iii) a multifrequency pulse consisting of the two pulses $p_{s0}(\pi,-\pi/2)$ and $p_{s1}(\pi,-\pi/2)$ to flip all the spins; (iv) a $p_{c(5/2)}(2\pi,\varphi)$ pulse with arbitrary phase, which affects only the phase factor of state $|1\rangle_c|\uparrow\rangle$; and (v) a multifrequency pulse consisting of the two pulses $p_{s0}(\pi,\pi/2)$ and $p_{s1}(\pi,\pi/2)$, which flips the spin states again.

For the sake of brevity, we do not show explicitly the intermediate steps of the above sequence. However, it is immediate to check that the generic two-qubit state

$$c_1|0\rangle_c|\downarrow\rangle + c_2|1\rangle_c|\downarrow\rangle + c_3|0\rangle_c|\uparrow\rangle + c_4|1\rangle_c|\uparrow\rangle \tag{75}$$

is turned into

$$c_1|0\rangle_c|\uparrow\rangle + c_2|1\rangle_c|\downarrow\rangle + c_3|0\rangle_c|\downarrow\rangle + c_4|1\rangle_c|\uparrow\rangle, \tag{76}$$

which is the desired result. We have, hence, proved how to implement also two-qubit operations with a single trapped electron.

To complete the Deutsch algorithm, one needs to apply once again the Hadamard transform $\mathcal{H}$ to both cyclotron and spin qubits, according to the prescription of Sec. V A. In the end, the readout of the first qubit state provides a conclusive answer to the question of whether the unknown Boolean function is constant or balanced.

However, before moving on to discuss the final measurement over the cyclotron and, optionally, spin qubit states, we would like to briefly mention an alternative implementation of the Deutsch algorithm. This second option relies on exchanging the roles of the cyclotron and of the spin: The latter is going to represent the first qubit, i.e., the controller, while the first becomes the target. The advantage here is that the transverse oscillating magnetic field may have a broader

bandwidth. Hence, even without selectively addressing the spin-flip frequencies, it remains possible to perform the required one- and two-qubit operations on both the spin and the cyclotron oscillator. The price to pay, however, is a slightly longer sequence of pulses to realize the NOT and CNOT gates, because of the not completely removed degeneracy between cyclotron transition frequencies.

VI. MEASURING THE QUBIT STATE

In order to measure the cyclotron and spin states, the homogeneous magnetic field of the trap is modified by a small additional field, the so-called magnetic bottle [13],

$$\Delta \mathbf{B} = B_2 \left[\left(z^2 - \frac{x^2+y^2}{2} \right) \hat{k} - z(x\hat{\imath} + y\hat{\jmath}) \right]. \tag{77}$$

This field couples the cyclotron and the spin motions to the axial oscillation producing a shift in the axial frequency depending on the cyclotron and spin quantum numbers, that is,

$$\delta\omega_z = \Delta\tilde{\omega}_z \left(\frac{gs}{4} + n + \frac{1}{2} \right), \tag{78}$$

where $\Delta\tilde{\omega}_z$ is a constant proportional to B_2. An alternative method [25] exploits, instead, the relativistic coupling between the different electronic degrees of freedom.

As a matter of fact, the axial motion is the only one easily detectable, because its characteristic frequency lies in the radio waves. To this purpose, the axial motion is driven by an alternated voltage applied to the trap electrodes. The oscillating electron induces a measurable current in the external circuit. Thanks to the extremely narrow line shape of the axial resonance, even frequency shifts of 1 Hz can be observed [12].

However, the magnetic bottle introduces an extra linewidth to cyclotron and spin transitions, because of the fluctuations fed in by the coupling with the axial motion. To prevent this unwanted effect, it is necessary to switch on the magnetic bottle only when all the operations on the qubits have been performed. This is possible if one uses a variable bottle, generated by superconducting loops, with the current induced by a flux transformer [13,26].

For simplicity, we take $g=2$ in Eq. (78). We see then that a spin flip and a change of 1 in the cyclotron number produce the same frequency shift $\Delta\tilde{\omega}_z/(2\pi) = 12.4$ Hz [12], which is much more than the experimental resolution. Hence, in reference to our scheme to implement the Deutsch algorithm, given that the spin leaves the network in its upper state, we can determine the cyclotron state $|n\rangle_c$ from the frequency shift in the axial oscillation.

In particular, the states of the two-qubit register, $|0\rangle_c|\downarrow\rangle$ and $|1\rangle_c|\uparrow\rangle$, correspond to different shifts of the axial frequency. Therefore, by measuring the axial resonance, we obtain complete information on both the qubits, i.e., we determine the cyclotron excitation and the spin state. Thus, in this case, we just need to monitor the oscillation frequency of the axial motion to read out the result of the computation and to check that the second qubit is truly returned to its initial state. This can be regarded as a very simple test of the correctness of the algorithm implementation.

Unfortunately, because of the smallness of the electron anomaly, to our knowledge it is not yet possible to resolve between the shifts produced by the two-qubit states $|1\rangle_c|\downarrow\rangle$ and $|0\rangle_c|\uparrow\rangle$. However, the spin state is usually [13] observed after a while, in order to allow the cyclotron motion to relax to its ground state. A continuous quantum-nondemolition (QND) observation of the cyclotron motion [12] enables us, then, to detect the eventual quantum jump from $|1\rangle_c$ to $|0\rangle_c$, which distinguishes between the two electronic states $|1\rangle_c|\downarrow\rangle$ and $|0\rangle_c|\uparrow\rangle$. Anyway, even without a QND measurement of the cyclotron state, this limitation is not so crucial for the Deutsch algorithm. Indeed, if no error takes place, the possible outcomes of the algorithm are represented by the pairs $|0\rangle_c|\uparrow\rangle$ or $|1\rangle_c|\uparrow\rangle$. Hence, within the current technology, one is always able to discriminate whether the Boolean function is constant or balanced.

VII. CONCLUSIONS

In this paper, we presented a method to implement the Deutsch algorithm using a single trapped electron. In our scheme, the qubits are stored in the first two cyclotron levels and in the electron spin. We exploit the small relativistic corrections to make the cyclotron motion anharmonic and selectively address specific transitions, by means of a tunable microwave source. Spin-flip transition frequencies are affected too by these relativistic corrections, so that they depend on the cyclotron quantum number *n*. This mutual interaction between cyclotron motion and spin is essential to realize two-qubit gates like the CNOT. However, we also mentioned an approach with less stringent requirements on the resolution of spin-flip transitions. Even without discriminating between different spin transition frequencies, one is able to perform the unitary operations required by the Deutsch algorithm. This is possible when the spin plays the role of the first qubit, while the cyclotron oscillator represents the second one.

We are aware that scalability is not so obvious in the system under consideration. However, the present proposal can provide proof of the principle of the validity of quantum logic operations and can be easily implemented with the present technology.

To increase the number of qubits, one may use the axial motion along the *z* axis of the trap. In typical experimental situations, this degree of freedom is in a classical regime, because of the interaction with the external detection circuit. However, it could be isolated from the environment by switching off the external measuring apparatus. At this stage, the axial motion is ready to be cooled down to its ground state by means of cavity sideband cooling. This is not such an irrelevant improvement, since with just three qubits one can implement a recently proposed algorithm [27], which is a variant on Grover's search [28]. Other options, to build up a larger quantum register, are presently under investigation. They rely on the anharmonic corrections to make use of more pairs of cyclotron and axial levels.

In conclusion, we feel it is worthwhile to realize this pro-

totype of a quantum computer. It may serve as a playground to test, at least, the simplest quantum algorithms, which require only one or two qubits [27]. To this end, we tried to model our theoretical proposal on the current technological and experimental possibilities.

ACKNOWLEDGMENTS

We are grateful to G. Gabrielse and S. Peil for stimulating and enlightening discussions on the experiments with an electron in the Penning trap.

[1] J.I. Cirac and P. Zoller, Phys. Rev. Lett. **74**, 4091 (1995).
[2] D. Jaksch, J.I. Cirac, P. Zoller, S.L. Rolston, R. Côté, and M.D. Lukin, Phys. Rev. Lett. **85**, 2208 (2000).
[3] T. Sleator and H. Weinfurter, Phys. Rev. Lett. **74**, 4087 (1995); Q.A. Turchette, C.J. Hood, W. Lange, H. Mabuchi, and H.J. Kimble, *ibid.* **75**, 4710 (1995); P. Domokos, J.M. Raimond, M. Brune, and S. Haroche, Phys. Rev. A **52**, 3554 (1995); V. Giovannetti, D. Vitali, P. Tombesi, and A. Ekert, *ibid.* **62**, 032306 (2000).
[4] For a review, see D.P. DiVincenzo, G. Burkard, D. Loss, and E.V. Sukhorukov, in *Quantum Mesoscopic Phenomena and Mesoscopic Devices in Microelectronics*, edited by I.O. Kulik and R. Ellialtioglu, NATO Advanced Study Institute Series C: Mathematical and Physical Sciences Vol. 559 (Kluwer, Dordrecht, 2000), e-print cond-mat/9911245.
[5] C. Monroe, D.M. Meekhof, B.E. King, W.M. Itano, and D.J. Wineland, Phys. Rev. Lett. **75**, 4714 (1995).
[6] C.A. Sackett, D. Kielpinski, B.E. King, C. Langer, V. Meyer, C.J. Myatt, M. Rowe, Q.A. Turchette, W.M. Itano, D.J. Wineland, and C. Monroe, Nature (London) **404**, 256 (2000).
[7] For a review, see J.A. Jones, Prog. NMR Spectrosc. **38**, 325 (2001).
[8] S.L. Braunstein, C.M. Caves, R. Jozsa, N. Linden, S. Popescu, and R. Schack, Phys. Rev. Lett. **83**, 1054 (1999).
[9] F.M. Penning, Physica (Amsterdam) **3**, 873 (1936).
[10] S. Mancini, A.M. Martins, and P. Tombesi, Phys. Rev. A **61**, 012303 (2000).
[11] R.S. Van Dyck, Jr., P. Schwinberg, and H. Dehmelt, Phys. Rev. Lett. **59**, 26 (1987).
[12] S. Peil and G. Gabrielse, Phys. Rev. Lett. **83**, 1287 (1999).
[13] L.S. Brown and G. Gabrielse, Rev. Mod. Phys. **58**, 233 (1986).
[14] G. Gabrielse (private communication).
[15] The name was suggested by H.G. Dehmelt.
[16] A.E. Kaplan, Phys. Rev. Lett. **48**, 138 (1982).
[17] G. Gabrielse, H.G. Dehmelt, and W. Kells, Phys. Rev. Lett. **54**, 537 (1985).
[18] G. Gabrielse and F.C. MacKintosh, Int. J. Mass Spectrom. Ion Phys. **57**, 1 (1984).
[19] J.N. Tan and G. Gabrielse, Appl. Phys. Lett. **55**, 2144 (1989).
[20] J.N. Tan and G. Gabrielse, Phys. Rev. Lett. **67**, 3090 (1991).
[21] G. Gabrielse and J. Tan, in *Advances Atomic, Molecular, and Optical Physics, Suppl. 2*, edited by P.R. Berman (Academic Press, San Diego, 1994), p. 267.
[22] J.D. Jackson, *Classical Electrodynamics* (Wiley, New York, 1975).
[23] D. Deutsch, Proc. R. Soc. London, Ser. A **400**, 97 (1985).
[24] R. Cleve, A. Ekert, C. Macchiavello, and M. Mosca, Proc. R. Soc. London, Ser. A **454**, 339 (1998).
[25] G. Gabrielse and H.G. Dehmelt, in *Precision Measurements and Fundamental Constants II*, edited by B.N. Taylor and W. D. Phillips, Natl. Bur. Stand. U.S. Spec. Publ. 617 (NBS, Washington, D.C., 1984), p. 219.
[26] P.B. Schwinberg, R.S. Van Dyck, Jr., and H.G. Dehmelt, Bull. Am. Phys. Soc. **24**, 1202 (1979).
[27] H.M. Wiseman and B.L. Hollis, e-print quant-ph/0009054.
[28] L.K. Grover, Phys. Rev. Lett. **79**, 325 (1997).